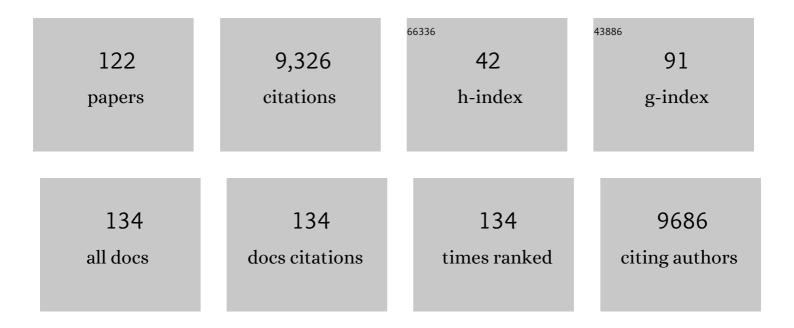
## **Pierrick Coupe**

List of Publications by Year in descending order

Source: https://exaly.com/author-pdf/8478251/publications.pdf Version: 2024-02-01



DIEDDICK COLIDE

#	Article	IF	CITATIONS
1	Microstructural Gray Matter Integrity Deteriorates After an Ischemic Stroke and Is Associated with Processing Speed. Translational Stroke Research, 2023, 14, 185-192.	4.2	2
2	DeepLesionBrain: Towards a broader deep-learning generalization for multiple sclerosis lesion segmentation. Medical Image Analysis, 2022, 76, 102312.	11.6	24
3	Deep learning based MRI contrast synthesis using full volume prediction using full volume prediction. Biomedical Physics and Engineering Express, 2022, 8, 015013.	1.2	0
4	A novel deep learning based hippocampus subfield segmentation method. Scientific Reports, 2022, 12, 1333.	3.3	6
5	Normal-Appearing White Matter Deteriorates over the Year After an Ischemic Stroke and Is Associated with Global Cognition. Translational Stroke Research, 2022, 13, 716-724.	4.2	3
6	Hippocampalâ€amygdaloâ€ventricular atrophy score: Alzheimer disease detection using normative and pathological lifespan models. Human Brain Mapping, 2022, 43, 3270-3282.	3.6	8
7	Structural progression of Alzheimer's disease over decades: the MRI staging scheme. Brain Communications, 2022, 4, fcac109.	3.3	35
8	Structural connectivity mapping in human hippocampal-subfields using super-resolution hybrid diffusion imaging: a feasibility study. Neuroradiology, 2022, , 1.	2.2	0
9	Deep Anomaly Generation: An Image Translation Approach of Synthesizing Abnormal Banded Chromosome Images. IEEE Access, 2022, 10, 59090-59098.	4.2	4
10	Cerebellar Atypicalities in Autism?. Biological Psychiatry, 2022, 92, 674-682.	1.3	20
11	vol2Brain: A New Online Pipeline for Whole Brain MRI Analysis. Frontiers in Neuroinformatics, 2022, 16, .	2.5	9
12	Multi-scale graph-based grading for Alzheimer's disease prediction. Medical Image Analysis, 2021, 67, 101850.	11.6	28
13	Deep correction of breathing-related artifacts in real-time MR-thermometry. Computerized Medical Imaging and Graphics, 2021, 87, 101834.	5.8	5
14	Deep Grading Based on Collective Artificial Intelligence for AD Diagnosis and Prognosis. Lecture Notes in Computer Science, 2021, , 24-33.	1.3	2
15	Distinct Hippocampal Subfields Atrophy in Older People With Vascular Brain Injuries. Stroke, 2021, 52, 1741-1750.	2.0	6
16	Grey and White Matter Volume Changes after Preterm Birth: A Meta-Analytic Approach. Journal of Personalized Medicine, 2021, 11, 868.	2.5	4
17	Toward a unified analysis of cerebellum maturation and aging across the entire lifespan: A <scp>MRI</scp> analysis. Human Brain Mapping, 2021, 42, 1287-1303.	3.6	19
18	Longitudinal study of functional brain network reorganization in clinically isolated syndrome. Multiple Sclerosis Journal, 2020, 26, 188-200.	3.0	17

#	Article	IF	CITATIONS
19	Normal-Appearing White Matter Integrity Is a Predictor of Outcome After Ischemic Stroke. Stroke, 2020, 51, 449-456.	2.0	24
20	Tensor-Based Grading: A Novel Patch-Based Grading Approach for the Analysis Of Deformation Fields in Huntington's Disease. , 2020, 2020, 1091-1095.		2
21	Accuracy of MRI Classification Algorithms in a Tertiary Memory Center Clinical Routine Cohort. Journal of Alzheimer's Disease, 2020, 74, 1157-1166.	2.6	19
22	Effect of cognitive rehabilitation on neuropsychological and semiecological testing and on daily cognitive functioning in multiple sclerosis: The REACTIV randomized controlled study. Journal of the Neurological Sciences, 2020, 415, 116929.	0.6	9
23	AssemblyNet: A large ensemble of CNNs for 3D whole brain MRI segmentation. NeuroImage, 2020, 219, 117026.	4.2	78
24	pBrain: A novel pipeline for Parkinson related brain structure segmentation. NeuroImage: Clinical, 2020, 25, 102184.	2.7	11
25	Differential annualized rates of hippocampal subfields atrophy in aging and future Alzheimer's clinical syndrome. Neurobiology of Aging, 2020, 90, 75-83.	3.1	28
26	RegQCNET: Deep quality control for image-to-template brain MRI affine registration. Physics in Medicine and Biology, 2020, 65, 225022.	3.0	14
27	Blind MRI Brain Lesion Inpainting Using Deep Learning. Lecture Notes in Computer Science, 2020, , 41-49.	1.3	9
28	Cerebellar parcellation in schizophrenia and bipolar disorder. Acta Psychiatrica Scandinavica, 2019, 140, 468-476.	4.5	24
29	Multimodal Hippocampal Subfield Grading For Alzheimer's Disease Classification. Scientific Reports, 2019, 9, 13845.	3.3	33
30	Lifespan Changes of the Human Brain In Alzheimer's Disease. Scientific Reports, 2019, 9, 3998.	3.3	113
31	Evolution of brain atrophy subtypes during aging predicts long-term cognitive decline and future Alzheimer's clinical syndrome. Neurobiology of Aging, 2019, 79, 22-29.	3.1	13
32	Regional hippocampal vulnerability in early multiple sclerosis: Dynamic pathological spreading from dentate gyrus to <scp>CA</scp> 1. Human Brain Mapping, 2018, 39, 1814-1824.	3.6	49
33	LesionBrain: An Online Tool for White Matter Lesion Segmentation. Lecture Notes in Computer Science, 2018, , 95-103.	1.3	17
34	MRI Denoising Using Deep Learning. Lecture Notes in Computer Science, 2018, , 12-19.	1.3	22
35	Differential Gray Matter Vulnerability in the 1 Year Following a Clinically Isolated Syndrome. Frontiers in Neurology, 2018, 9, 824.	2.4	12
36	Adaptive fusion of texture-based grading for Alzheimer's disease classification. Computerized Medical Imaging and Graphics, 2018, 70, 8-16.	5.8	44

#	Article	IF	CITATIONS
37	MRI white matter lesion segmentation using an ensemble of neural networks and overcomplete patch-based voting. Computerized Medical Imaging and Graphics, 2018, 69, 43-51.	5.8	32
38	Antipsychotic and benzodiazepine use and brain morphology in schizophrenia and affective psychoses – Systematic reviews and birth cohort study. Psychiatry Research - Neuroimaging, 2018, 281, 43-52.	1.8	3
39	Comparing fully automated state-of-the-art cerebellum parcellation from magnetic resonance images. NeuroImage, 2018, 183, 150-172.	4.2	80
40	Graph of Hippocampal Subfields Grading for Alzheimer's Disease Prediction. Lecture Notes in Computer Science, 2018, , 259-266.	1.3	5
41	Graph of Brain Structures Grading for Early Detection of Alzheimer's Disease. Lecture Notes in Computer Science, 2018, , 429-436.	1.3	4
42	Posterior lobules of the cerebellum and information processing speed at various stages of multiple sclerosis. Journal of Neurology, Neurosurgery and Psychiatry, 2017, 88, 146-151.	1.9	52
43	A comparison of accurate automatic hippocampal segmentation methods. NeuroImage, 2017, 155, 383-393.	4.2	35
44	Long-term antipsychotic and benzodiazepine use and brain volume changes in schizophrenia: The Northern Finland Birth Cohort 1966 study. Psychiatry Research - Neuroimaging, 2017, 266, 73-82.	1.8	21
45	SuperPatchMatch: An Algorithm for Robust Correspondences Using Superpixel Patches. IEEE Transactions on Image Processing, 2017, 26, 4068-4078.	9.8	31
46	HIPS: A new hippocampus subfield segmentation method. NeuroImage, 2017, 163, 286-295.	4.2	56
47	Early Prediction of Alzheimer's Disease with Non-local Patch-Based Longitudinal Descriptors. Lecture Notes in Computer Science, 2017, , 74-81.	1.3	3
48	Adaptive Fusion of Texture-Based Grading: Application to Alzheimer's Disease Detection. Lecture Notes in Computer Science, 2017, , 82-89.	1.3	4
49	Hippocampus Subfield Segmentation Using a Patch-Based Boosted Ensemble of Autocontext Neural Networks. Lecture Notes in Computer Science, 2017, , 29-36.	1.3	3
50	Towards a unified analysis of brain maturation and aging across the entire lifespan: A MRI analysis. Human Brain Mapping, 2017, 38, 5501-5518.	3.6	209
51	M89. Long-Term Antipsychotic and Benzodiazepine Use and Brain Volume Changes in Schizophrenia: The Northern Finland Birth Cohort 1966 Study. Schizophrenia Bulletin, 2017, 43, S243-S243.	4.3	Ο
52	CERES: A new cerebellum lobule segmentation method. NeuroImage, 2017, 147, 916-924.	4.2	133
53	Hippocampal microstructural damage correlates with memory impairment in clinically isolated syndrome suggestive of multiple sclerosis. Multiple Sclerosis Journal, 2017, 23, 1214-1224.	3.0	52
54	[P2–379]: ACCURACY OF MRI CLASSIFICATION ALGORITHMS IN A TERTIARY MEMORY CENTER CLINICAL ROUTINE COHORT. Alzheimer's and Dementia, 2017, 13, P772.	0.8	1

#	Article	IF	CITATIONS
55	Microstructural analyses of the posterior cerebellar lobules in relapsing-onset multiple sclerosis and their implication in cognitive impairment. PLoS ONE, 2017, 12, e0182479.	2.5	11
56	A patch-based framework for new ITK functionality: Joint fusion, denoising, and non-local super-resolution. The Insight Journal, 2017, , .	0.2	1
57	Optic Radiations Microstructural Changes in Glaucoma and Association With Severity: A Study Using 3Tesla-Magnetic Resonance Diffusion Tensor Imaging. , 2016, 57, 6539.		22
58	volBrain: An Online MRI Brain Volumetry System. Frontiers in Neuroinformatics, 2016, 10, 30.	2.5	379
59	Lifetime antipsychotic use and brain structures in schizophrenia and other psychoses – 43-year study of the Northern Finland Birth Cohort 1966. European Psychiatry, 2016, 33, S100-S101.	0.2	0
60	Patch-Based DTI Grading: Application to Alzheimer's Disease Classification. Lecture Notes in Computer Science, 2016, , 76-83.	1.3	6
61	High Resolution Hippocampus Subfield Segmentation Using Multispectral Multiatlas Patch-Based Label Fusion. Lecture Notes in Computer Science, 2016, , 117-124.	1.3	6
62	Non-local MRI Library-Based Super-Resolution: Application to Hippocampus Subfield Segmentation. Lecture Notes in Computer Science, 2016, , 68-75.	1.3	1
63	Automatic thalamus and hippocampus segmentation from MP2RAGE: comparison of publicly available methods and implications for DTI quantification. International Journal of Computer Assisted Radiology and Surgery, 2016, 11, 1979-1991.	2.8	40
64	Non Local Spatial and Angular Matching: Enabling higher spatial resolution diffusion MRI datasets through adaptive denoising. Medical Image Analysis, 2016, 32, 115-130.	11.6	61
65	Early Fiber Number Ratio Is a Surrogate of Corticospinal Tract Integrity and Predicts Motor Recovery After Stroke. Stroke, 2016, 47, 1053-1059.	2.0	63
66	An Optimized PatchMatch for multi-scale and multi-feature label fusion. NeuroImage, 2016, 124, 770-782.	4.2	68
67	HIST: HyperIntensity Segmentation Tool. Lecture Notes in Computer Science, 2016, , 92-99.	1.3	5
68	Sparse-Based Morphometry: Principle and Application to Alzheimer's Disease. Lecture Notes in Computer Science, 2016, , 43-50.	1.3	1
69	ICâ€₽â€099: A quantitative comparison between two manual hippocampal segmentation protocols. Alzheimer's and Dementia, 2015, 11, P67.	0.8	1
70	Detection of Alzheimer's disease signature in MR images seven years before conversion to dementia: Toward an early individual prognosis. Human Brain Mapping, 2015, 36, 4758-4770.	3.6	52
71	Non-Local Means Inpainting of MS Lesions in Longitudinal Image Processing. Frontiers in Neuroscience, 2015, 9, 456.	2.8	19
72	Rotation-invariant multi-contrast non-local means for MS lesion segmentation. NeuroImage: Clinical, 2015, 8, 376-389.	2.7	56

#	Article	IF	CITATIONS
73	Standardized evaluation of algorithms for computer-aided diagnosis of dementia based on structural MRI: The CADDementia challenge. NeuroImage, 2015, 111, 562-579.	4.2	266
74	MRI noise estimation and denoising using non-local PCA. Medical Image Analysis, 2015, 22, 35-47.	11.6	138
75	Structural imaging biomarkers of Alzheimer's disease: predicting disease progression. Neurobiology of Aging, 2015, 36, S23-S31.	3.1	101
76	NABS: non-local automatic brain hemisphere segmentation. Magnetic Resonance Imaging, 2015, 33, 474-484.	1.8	25
77	Patch-Based Segmentation from MP2RAGE Images: Comparison to Conventional Techniques. Lecture Notes in Computer Science, 2015, , 180-187.	1.3	2
78	Nonlocal Intracranial Cavity Extraction. International Journal of Biomedical Imaging, 2014, 2014, 1-11.	3.9	49
79	IC-P-150: A UNIFIED ASSESSMENT OF FULLY AUTOMATED HIPPOCAMPUS SEGMENTATION METHODS. , 2014, 10 P86-P86.	,	2
80	Nonlocal regularization for active appearance model: Application to medial temporal lobe segmentation. Human Brain Mapping, 2014, 35, 377-395.	3.6	20
81	Optimized PatchMatch for Near Real Time and Accurate Label Fusion. Lecture Notes in Computer Science, 2014, 17, 105-112.	1.3	31
82	Anatomically Constrained Weak Classifier Fusion for Early Detection of Alzheimer's Disease. Lecture Notes in Computer Science, 2014, , 141-148.	1.3	6
83	A new method for structural volume analysis of longitudinal brain MRI data and its application in studying the growth trajectories of anatomical brain structures in childhood. NeuroImage, 2013, 82, 393-402.	4.2	145
84	Volumetric analysis of medial temporal lobe structures in brain development from childhood to adolescence. Neurolmage, 2013, 74, 276-287.	4.2	91
85	Collaborative patch-based super-resolution for diffusion-weighted images. NeuroImage, 2013, 83, 245-261.	4.2	83
86	Automated segmentation of basal ganglia and deep brain structures in MRI of Parkinson's disease. International Journal of Computer Assisted Radiology and Surgery, 2013, 8, 99-110.	2.8	57
87	Segmentation of MR images via discriminative dictionary learning and sparse coding: Application to hippocampus labeling. NeuroImage, 2013, 76, 11-23.	4.2	196
88	Prediction of Alzheimer's disease in subjects with mild cognitive impairment from the ADNI cohort using patterns of cortical thinning. NeuroImage, 2013, 65, 511-521.	4.2	224
89	Diffusion Weighted Image Denoising Using Overcomplete Local PCA. PLoS ONE, 2013, 8, e73021.	2.5	299
90	3D Rigid Registration of Intraoperative Ultrasound and Preoperative MR Brain Images Based on Hyperechogenic Structures. International Journal of Biomedical Imaging, 2012, 2012, 1-14.	3.9	31

#	Article	IF	CITATIONS
91	Adaptive multiresolution non-local means filter for three-dimensional magnetic resonance image denoising. IET Image Processing, 2012, 6, 558.	2.5	84
92	Scoring by nonlocal image patch estimator for early detection of Alzheimer's disease. NeuroImage: Clinical, 2012, 1, 141-152.	2.7	104
93	BEaST: Brain extraction based on nonlocal segmentation technique. NeuroImage, 2012, 59, 2362-2373.	4.2	507
94	Simultaneous segmentation and grading of anatomical structures for patient's classification: Application to Alzheimer's disease. NeuroImage, 2012, 59, 3736-3747.	4.2	129
95	Validation of a hybrid Doppler ultrasound vessel-based registration algorithm for neurosurgery. International Journal of Computer Assisted Radiology and Surgery, 2012, 7, 667-685.	2.8	17
96	New methods for MRI denoising based on sparseness and self-similarity. Medical Image Analysis, 2012, 16, 18-27.	11.6	224
97	A CANDLE for a deeper in vivo insight. Medical Image Analysis, 2012, 16, 849-864.	11.6	58
98	A New Framework for Analyzing Structural Volume Changes of Longitudinal Brain MRI Data. Lecture Notes in Computer Science, 2012, , 50-62.	1.3	0
99	Appearance-based modeling for segmentation of hippocampus and amygdala using multi-contrast MR imaging. NeuroImage, 2011, 58, 549-559.	4.2	35
100	Patch-based segmentation using expert priors: Application to hippocampus and ventricle segmentation. NeuroImage, 2011, 54, 940-954.	4.2	692
101	Real time ultrasound image denoising. Journal of Real-Time Image Processing, 2011, 6, 15-22.	3.5	55
102	Simultaneous Segmentation and Grading of Hippocampus for Patient Classification with Alzheimer's Disease. Lecture Notes in Computer Science, 2011, 14, 149-157.	1.3	9
103	An automatic geometrical and statistical method to detect acoustic shadows in intraoperative ultrasound brain images. Medical Image Analysis, 2010, 14, 195-204.	11.6	26
104	Non-local MRI upsampling. Medical Image Analysis, 2010, 14, 784-792.	11.6	218
105	Adaptive nonâ€local means denoising of MR images with spatially varying noise levels. Journal of Magnetic Resonance Imaging, 2010, 31, 192-203.	3.4	823
106	Robust Rician noise estimation for MR images. Medical Image Analysis, 2010, 14, 483-493.	11.6	200
107	Intraoperative ultrasonography for the correction of brainshift based on the matching of hyperechogenic structures. , 2010, , .		1
108	MRI Superresolution Using Self-Similarity and Image Priors. International Journal of Biomedical Imaging, 2010, 2010, 1-11.	3.9	79

#	Article	IF	CITATIONS
109	Robust 3D Reconstruction and Mean-Shift Clustering of Motoneurons from Serial Histological Images. Lecture Notes in Computer Science, 2010, , 191-199.	1.3	2
110	Nonlocal Patch-Based Label Fusion for Hippocampus Segmentation. Lecture Notes in Computer Science, 2010, 13, 129-136.	1.3	36
111	Nonlocal means-based speckle filtering for ultrasound images. IEEE Transactions on Image Processing, 2009, 18, 2221-2229.	9.8	502
112	An Object-Based Method for Rician Noise Estimation in MR Images. Lecture Notes in Computer Science, 2009, 12, 601-608.	1.3	3
113	An Optimized Blockwise Nonlocal Means Denoising Filter for 3-D Magnetic Resonance Images. IEEE Transactions on Medical Imaging, 2008, 27, 425-441.	8.9	973
114	Rician Noise Removal by Non-Local Means Filtering for Low Signal-to-Noise Ratio MRI: Applications to DT-MRI. Lecture Notes in Computer Science, 2008, 11, 171-179.	1.3	157
115	Bayesian non local means-based speckle filtering. , 2008, , .		62
116	Acoustic shadows detection, application to accurate reconstruction of 3D intraoperative ultrasound. , 2008, , .		3
117	3D Wavelet Subbands Mixing for Image Denoising. International Journal of Biomedical Imaging, 2008, 2008, 1-11.	3.9	65
118	A PROBABILISTIC OBJECTIVE FUNCTION FOR 3D RIGID REGISTRATION OF INTRAOPERATIVE US AND PREOPERATIVE MR BRAIN IMAGES. , 2007, , .		8
119	Non-Local Means Variants for Denoising of Diffusion-Weighted and Diffusion Tensor MRI. Lecture Notes in Computer Science, 2007, 10, 344-351.	1.3	52
120	Probe trajectory interpolation for 3D reconstruction of freehand ultrasound. Medical Image Analysis, 2007, 11, 604-615.	11.6	23
121	Simulation of Biphasic CT Findings in Hepatic Cellular Carcinoma by a Two-Level Physiological Model. IEEE Transactions on Biomedical Engineering, 2007, 54, 538-542.	4.2	14
122	Bayesian Non-local Means Filter, Image Redundancy and Adaptive Dictionaries for Noise Removal. , 2007, , 520-532.		144